

Available online at www.sciencedirect.com

## SciVerse ScienceDirect

Acta Materialia 59 (2011) 7498-7507



www.elsevier.com/locate/actamat

# Atomic transport mechanisms in thin oxide films grown on zirconium by thermal oxidation, as-derived from <sup>18</sup>O-tracer experiments

G. Bakradze<sup>a</sup>, L.P.H. Jeurgens<sup>a,\*</sup>, T. Acartürk<sup>b</sup>, U. Starke<sup>b</sup>, E.J. Mittemeijer<sup>a,c</sup>

<sup>a</sup> Max Planck Institute for Intelligent Systems (Formerly Max Planck Institute for Metals Research), Heisenbergstraße 3, D-70569 Stuttgart, Germany

<sup>b</sup> Max Planck Institute for Solid State Research, Heisenbergstraße 1, D-70569 Stuttgart, Germany

<sup>c</sup> Institute for Materials Science, University of Stuttgart, Germany

Received 20 May 2011; received in revised form 5 August 2011; accepted 23 August 2011 Available online 15 October 2011

#### Abstract

Two-stage oxidation experiments using  $^{16}O$  and  $^{18}O$  isotopes were performed to reveal the governing atomic transport mechanism(s) in thin (thickness <10 nm) oxide films grown during the initial stages of dry thermal oxidation of pure Zr at 450 K. To this end, bare (i.e. without a native oxide) Zr(0001) and Zr(1010) single-crystalline surfaces were prepared under ultra-high vacuum conditions by a cyclic treatment of alternating ion-sputtering and in vacuo annealing steps. Next, the bare Zr surfaces were oxidized at 450 K and at  $pO_2 = 1 \times 10^{-4}$  Pa, first in  $^{16}O_2(g)$  and subsequently in  $^{18}O_2(g)$ . The  $^{18}O$ -tracer depth distributions in the oxide films were recorded by time-of-flight secondary ion mass spectrometry. It was concluded that the early stage of the oxidation process is governed by oxygen transport to the metal/oxide interface through the lattice and along the grain boundaries of the nanosized oxide grains whereas, on continuing oxidation, only oxygen lattice transport controls the oxidation process. An oxide-film growth mechanism is proposed. © 2011 Acta Materialia Inc. Published by Elsevier Ltd. All rights reserved.

Keywords: Oxidation; Mechanism; Nanocrystalline films; Zirconium; Time-of-flight secondary ion mass-spectrometry

#### 1. Introduction

In many application areas, such as powder metallurgy, microelectronics, gas sensors, surface coatings and catalysis, comprehensive knowledge of the atomic transport phenomena in thin oxide layers is a prerequisite in order to control and optimize the functional properties of metallicand/or semiconductor-based components under varying operating conditions [1–6]. Fundamental investigations on the transport mechanisms in oxide films, such as developing on metal and alloy surfaces by, for example, thermal oxidation, should particularly address: (i) the type of (rate-determining) migrating species (anions, cations and the corresponding vacancies, as well as electrons and electron holes) and the associated reaction fronts (e.g. oxide/gas and/or metal/oxide interface), as well as (ii) the transport

paths (e.g., lattice vs. grain-boundary transport) and transport mechanisms (e.g. vacancy, interstitial, substitutional) of the migrating species. The quantitative, direct experimental assessment of (iii) the rate of the migrating species (e.g. diffusivities) [7] and (iv) the (steady-state) defect concentrations at the metal/oxide and oxide/gas interfaces presents a considerable experimental challenge, particularly for very thin (thickness <10 nm) oxide films, as dealt with in the present study, and is beyond the scope of this work.

In the past, several types of marker and tracer experiments were designed to identify the predominant transport species during surface oxidation, in particular by determining the reaction front(s) of the oxidation reaction [8–11]. For example, in a so-called "two-stage oxidation experiment", when the substrate is first oxidized in a "natural"  $^{16}O_2(g)$  atmosphere and subsequently in a "labelled" (but chemically identical)  $^{18}O_2(g)$  atmosphere; the following determination of the specific distribution of the  $^{18}O$  tracer in the grown oxide layer can disclose the more mobile species in the oxidation process. Determination of such

<sup>\*</sup> Corresponding author. Tel.: +49 711 6893485; fax: +49 711 6893312. E-mail address: jeurgens@is.mpg.de (L.P.H. Jeurgens).

isotope depth distributions in thin films requires a high depth resolution, which can be offered by a mass-sensitive surface-analytical technique as time-of-flight secondary ion mass spectrometry (ToF-SIMS) or nuclear reaction analysis. From the established depth profiles of the fraction of the <sup>18</sup>O-tracer component  $c(\tau)$  (see Section 2.4 for details), the predominant transport mechanisms during the oxidation process can be deduced by considering the various possible cases for the governing transport mechanism as follows (see Fig. 1) [9,12].

If outward metal transport is the governing mechanism during the second oxidation step performed in a pure <sup>18</sup>O<sub>2</sub>(g) atmosphere, an <sup>18</sup>O-rich oxide will be formed preferentially at the gas/oxide interface, and the  $c(\tau)$  profile will resemble Fig. 1a. If inward oxygen transport predominates during the second oxidation step, the shape of the  $c(\tau)$  profile will depend on the particular oxygen transport path: (i) if O is transported through the oxide lattice by a vacancy mechanism or by an interstitial mechanism (which is unlikely), the  $c(\tau)$  profile will look like Fig. 1b, whereas (ii) for inward O transport through short-circuits (e.g. through grain boundaries (GB) or cracks), <sup>18</sup>O-rich oxide will form mainly near the oxide/metal interface (see Fig. 1c). In general, isotopic exchange at oxide GB cannot be neglected and, consequently, the  $c(\tau)$  profile for case (ii) (see Fig. 1c) will rather resemble that of Fig. 1d. A combination of the above-described predominant transport mechanisms typically results in more complicated shapes of the measured  $c(\tau)$  profiles [9,12–14], as encountered in the present study (see Section 4).

To date, two-stage oxidation experiments, as sketched above, have been conducted mainly for the case of growth of micrometre-thick (crystalline) oxide scales, e.g. as grown

by thermal oxidation at elevated temperatures (T > 700 K) on pure Ni [12,15], pure Cr and Al [16], NiAl intermetallics and Ni-Cr-Al-Y alloys [17]. Fe-Cr alloy and zircaloy-4 [12], zirconium [18] and zirconium—tin alloys [19]. The present work aims to apply two-stage oxidation experiments to the case of growth of very thin (thickness <10 nm) oxide overgrowths, as developing at low temperatures up to  $\sim$ 500 K [20,21]. Further, in this way, the present <sup>18</sup>O-tracer oxidation study is meant to clarify an existing controversy in the literature regarding the governing mechanism for the low-temperature oxidation of Zr: as proposed in Ref. [22]. the low-temperature oxidation rate of Zr would be limited by either inward O transport or the dissociative chemisorption of O<sub>2</sub>(g) at the oxide surface, whereas according to Ref. [23] outward cation transport would be the rate-limiting step in the oxidation process. Understanding the oxidation mechanism(s) of Zr in the low-temperature regime is not only of great importance for applications of very thin Zr-oxide layers in state-of-the-art nanotechnologies and microelectronics, but also to complement existing knowledge on the corrosion resistance and embrittlement of Zr (and its alloys) in conventional nuclear cladding applications [24-26].

In the present study, single-crystalline Zr(0001) and  $Zr(10\bar{1}0)$  surfaces were oxidized by successive exposures (for different times) to  $^{16}O_2(g)$  and  $^{18}O_2(g)$  at 450 K and at a partial oxygen pressure of  $pO_2=1\times 10^{-4}$  Pa. ToF-SIMS was applied to establish the  $^{18}O$ -tracer-depth profiles in the grown oxide films (Section 2). On the basis of the identified governing transport mechanisms at different stages of the oxidation process (Section 4), a corresponding, overall oxide-film growth mechanism is proposed for the oxidation at 450 K (Section 5). Details of the growth

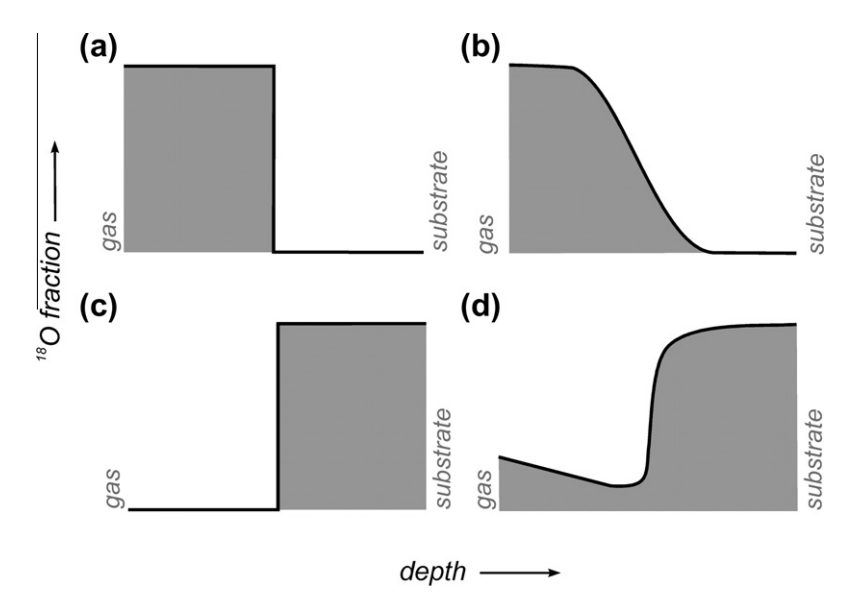


Fig. 1. Schematic O-tracer depth distribution profiles in an oxide layer, as grown under control of different (combinations of) transport processes (after Refs. [8,9,12]): (a) outward metal transport (either through the lattice or along short-circuits); (b) inward oxygen transport by a vacancy (or interstitial) mechanism; (c) inward oxygen short-circuit transport (without isotope exchange); (d) inward oxygen short-circuit transport with isotope exchange. See Section 1 for details.

### Download English Version:

# https://daneshyari.com/en/article/10620345

Download Persian Version:

 $\underline{https://daneshyari.com/article/10620345}$ 

Daneshyari.com